temperature the rate of tunneling is still larger than the classical rate by 3 orders of magnitude. Even though the rate calculated from the transmission probability is necessarily smaller than the rate derived from the energy splitting, we now show that with the same parameters one may still reach the same conclusion concerning the role of tunneling. The two rates at zero temperature can be written[6] in terms of the transmission probability T and the frequency of the promoting mode ν_F

$$k^0_{TP} = \nu_F T \qquad k^0_{ES} = \frac{2\nu_F}{\Pi} T^{1/2} \tag{7}$$

or alternatively, introducing the energy splitting ΔE_0

$$k^0_{TP} = \frac{1}{4}\frac{(\Delta E_0)^2}{\hbar^2 \nu_F} \qquad k^0_{ES} = \frac{2\Delta E_0}{h} \tag{8}$$

The energy splitting enters k_{TP} through the transmission probability T. With the parameters of Dewar et al.[4] (barrier height, frequency of promoting mode) and their method for calculating the energy splitting, we obtain $k^0_{TP} = 1.4 \times 10^{10}\ s^{-1}$. This is still two orders of magnitude larger than their classical rate.

Carpenter in his original work[1] obtained a much lower value for the tunneling rate estimated from the transmission probability ($k^0_{TP} \simeq 8 \times 10^4\ s^{-1}$). We reconsider the calculation of this rate performed with a truncated parabolic barrier. With a reduced mass of 13 daltons to model the motion of the pseudoatoms, a barrier height equal to that of Dewar et al.[4] (8.14 kcal/mol), and a frequency of the promoting mode taken from Čarsky et al.[5] ($\nu_F = 4.7 \times 10^{13}$ Hz), we obtain $k^0_{TP} = 2.85 \times 10^8\ s^{-1}$. This is much closer to the other estimates and allows us to conclude that there is a significant contribution from tunneling to the overall rate even if one accepts the classical estimate of Dewar et al.[4]

To summarize, first-order kinetics can only be obtained in the tunneling problem if one takes into account the relaxation in the final configuration of the system. This is in favor of the method based on a transmission probability which agrees with the concept of decay rate as being a probability per second (k_{TP} is a first-order rate constant while k_{ES} is not).

Acknowledgment. We thank the Referees for helping to improve the original version of the paper. This research is supported in part by the US-Israel Binational Foundation. One of us (R.L.) is grateful for the invitation extended to him by the Chemistry Department of Technion, Haifa.

Registry No. Cyclobutadiene, 1120-53-2.

Ab Initio Spin-Coupled Description of the Reactions $CH_2(^1A_1) + H_2 \rightarrow CH_4$ and $CH_4 \rightarrow CH_3(^2A_1') + H$

Maurizio Sironi,*[1a] David L. Cooper,*[1b] Joseph Gerratt,[1c] and Mario Raimondi[1a]

Contribution from the Dipartimento di Chimica Fisica ed Elettrochimica, Università di Milano, Via Golgi 19, 20133 Milano, Italy, Department of Chemistry, University of Liverpool, P.O. Box 147, Liverpool L69 3BX, UK, and Department of Theoretical Chemistry, University of Bristol, Cantocks Close, Bristol BS8 1TS, UK. *Received June 19, 1989*

Abstract: Spin-coupled theory, which represents the modern development of valence bond theory, is applied to the singlet methylene insertion reaction $CH_2(^1A_1) + H_2 \rightarrow CH_4$ and to the hydrogen atom abstraction reaction $CH_4 \rightarrow CH_3(^2A_1') + H$. The spin-coupled wave function provides a highly visual model of the behavior of *correlated* electrons. Concepts such as directed covalent bonds, formed from the overlap of sp^x-like hybrids on carbon and 1s functions on hydrogen, are shown to arise naturally from minimizing the total energy without preconceptions. There are, however, some important differences from the ideas of classical VB theory. A new non-least-motion pathway with no activation barrier is proposed for the singlet methylene insertion reaction.

I. Introduction

The methane molecule is of fundamental importance to the whole of organic chemistry, and its elementary reactions are an obvious testing ground for any theory of chemical reactivity. In particular, the two connected potential energy surfaces

$$CH_2(^1A_1) + H_2 \rightarrow CH_4$$

and

$$CH_4 \rightarrow CH_3(^2A_1') + H$$

are of special importance as providing the simplest examples of singlet methylene insertion and of hydrogen atom abstraction reactions. The second reaction involves the breaking of a single bond only and is a relatively straightforward process. However, the singlet methylene insertion reaction is altogether much more complicated and is a prototype for a wide range of chemical processes.

The aim of the present work is to provide reliable orbital pictures for both reaction mechanisms and to understand the changes that occur in the coupling of the electron spins. We show that concepts such as directed covalent bonds, formed from the overlap of sp^x-like hybrids on carbon and 1s functions on hydrogen, arise naturally from our ab initio calculations simply by minimizing the energy without preconceptions. There are, however, some important differences from classical VB descriptions.

The central result of this paper is that our orbital picture for singlet methylene allows us to suggest a new non-least-motion pathway with no activation barrier for singlet methylene insertion. This reaction is very interesting from a theoretical point of view, as it involves the complex process of forming two new C-H bonds while breaking the strong bond in H_2. We examine least-motion and non-least-motion paths across this portion of the potential surface. For the hydrogen atom abstraction reaction, we concentrate on a least-motion path. A detailed dynamical treatment of both reactions, based on classical trajectories or on quantum scattering calculations, would require a rather more extensive study of the potential energy surfaces. However, such dynamical studies would be unlikely, on their own, to give detailed pictures of the

(1) (a) Università di Milano. (b) University of Liverpool. (c) University of Bristol.

0002-7863/90/1512-5054$02.50/0

bond-breaking and bond-forming processes at an electronic structure level. In any case, quantum scattering theory is not yet able to treat the dynamics of a reaction as complex as the singlet methylene insertion process.

The structure of this paper is as follows. In the next section we mention very briefly some of the drawbacks of MO-based methods and of classical VB theory, in order to make it clear why we have chosen to use spin-coupled theory in the present work. Section III provides an overview of those features of spin-coupled theory that are most relevant to the present study. The calculations and the spin-coupled wave functions for $CH_2(^1A_1)$, CH_4, H_2, and CH_3 are described in section IV, and our results are presented in section V. These are discussed in section VI and compared with classical VB theory. Finally, we present a summary and our conclusions in section VII and identify possible directions for future work.

II. Approaches to Molecular Electronic Structure

For more than 30 years, our fundamental understanding of molecular electronic structure has been based in the most part on molecular orbital (MO) theory. According to the Hartree–Fock self-consistent-field (SCF) model, the electrons move more or less independently of one another, experiencing only the time-averaged effects of the electron–electron interactions. This approach has many serious failings, not least of which is the difficulty of connecting the molecular configurations with the asymptotic atomic or molecular fragment states. In addition, the Hartree–Fock model breaks down for almost all bond-dissociation processes; the inclusion of the effects of electron correlation is crucial in some cases even to attain a qualitatively correct description near the equilibrium geometry. Electron correlation can, of course, be included with use of a variety of configuration interaction (CI) techniques, but the interpretation of multiconfiguration wave functions can be very difficult. Particularly with the very long lists of configurations used in contemporary calculations, the loss of any useful visual model of the wave function is almost complete.

From the point of view of the requirement for a reliable quantitative *and* qualitative picture of molecular processes, the straightforward *ab initio* application of classical valence bond (VB) theory has always appeared to be an attractive alternative to MO theory. Unfortunately, the rate of convergence with the number of VB structures is disconcertingly slow. This is especially true when the large atomic basis sets that are required for high accuracy within any ab initio approach are used. Worse still is the intervention of large numbers of ionic structures, even in evidently covalent situations such as hydrocarbon fragments. The physical reason for the *apparent* high importance of ionic structures is very clear. When two fragments approach one another, we should expect a degree of distortion of their respective wave functions. At an orbital level, this can occur by mixing together the different atomic functions on the same center and also by a small amount of delocalization onto other centers. However, the orbitals in classical VB theory are each constrained to be localized about just one atomic center. This is quite insufficient for all the necessary deformations to occur in the classical VB covalent structure. Consequently, there is a significant contribution by the ionic structures to compensate for this.

A significant number of classical VB structures is required in most cases merely to match the energy from a Hartree–Fock SCF calculation with the same atomic basis set. Leaving aside the question of ionic structures, the long lists of classical VB structures required for high accuracy presents problems of interpretation similar to those of MO–CI techniques.

In the present work we employ a general approach based on spin-coupled theory, which represents VB theory in its modern form, to provide a uniform description of the two connected surfaces. This approach provides a highly visual model of the behavior of *correlated* electrons. The spin-coupled wave function for an N-electron system is based on a picture of N singly occupied orbitals, with one orbital for each electron. Each of the orbitals is allowed to overlap freely with each of the others. The orbitals are fully optimized by expanding them in an atomic basis set without preconceptions as to the degree of localization and without constraints on their symmetry properties. Furthermore, the spin-coupled wave function is not invariant to arbitrary linear transformations of the orbitals, so that their form is a *unique* outcome of the variational procedure.

The non-orthogonality and single occupancy of the orbitals have the important consequence that there is almost always more than one way in which the individual spins of the N electrons can be coupled together so as to achieve the required total spin of the molecule. In general, all of these are included, and their weights are fully optimized simultaneously with the form of the orbitals, so as to minimize the total energy. The spin-coupled wave function represents the most general description of electronic structure in terms of a single orbital configuration. The non-orthogonality of the orbitals, together with the inclusion of all the spin degrees of freedom, allows us to describe properly all of the possible modes of dissociation of the system. Special cases of the spin-coupled wave function may be obtained by imposing various constraints in the calculation, and these include the restricted Hartree–Fock SCF and the perfect-pairing GVB wave functions.

Of course, the spin-coupled wave function is not an exact solution of the electronic Schrödinger problem. It does, however, include a significant amount of correlation. Moreover, it describes correctly all bond-formation and bond-breaking processes, no matter how complicated. Further correlation can be incorporated by including additional structures in a non-orthogonal CI calculation. Three important findings, which emerge from a very large number of applications of this approach, are that fairly short lists of configurations are sufficient to achieve very high accuracy, that the resource requirements compare favorably with those of MO–CI procedures, *and* that the final wave function is overwhelmingly dominated by the spin-coupled configuration for all nuclear geometries. In other words, the further refinement of the spin-coupled wave function does not change the essential physical picture. Consequently, we may claim that the spin-coupled valence bond approach to molecular electronic structure combines high accuracy with ease of interpretation.

In the next section, we present a brief overview of those features of spin-coupled VB theory that are most relevant to our investigation of the reactions $CH_2(^1A_1) + H_2 \rightarrow CH_4$ and $CH_4 \rightarrow CH_3(^2A_1') + H$. A number of recent reviews are available,[2-6] and the interested reader is referred to these and to the literature cited.

III. Spin-Coupled Valence-Bond Theory

We start by considering a complete set of spin functions $\Theta^N_{SM;k}$ for a system of N electrons with total spin S and projection M:

$$\hat{S}^2\Theta^N_{SM;k} = S(S+1)\hbar^2\Theta^N_{SM;k}$$

and

$$\hat{S}_z\Theta^N_{SM;k} = M\hbar\Theta^N_{SM;k} \tag{1}$$

For each value of M there are f^N_S linearly independent spin functions, labeled by the index k, where

$$f^N_S = \frac{(2S+1)N!}{(\frac{1}{2}N+S+1)!(\frac{1}{2}N-S)!} \tag{2}$$

The exact solution Ψ_{SM} of the electronic structure problem can be written in the form[7-9]

(2) Cooper, D. L.; Gerratt, J.; Raimondi, M. *Adv. Chem. Phys.* **1987**, *69*, 319.
(3) Cooper, D. L.; Gerratt, J.; Raimondi, M. *Int. Rev. Phys. Chem.* **1988**, *7*, 59.
(4) (a) Gerratt, J.; Cooper, D. L.; Raimondi, M. In *Valence Bond Theory and Chemical Structure*; Klein, D. J., Trinajstič, N., Eds.; Elsevier: 1990. (b) Raimondi, M.; Sironi, M., ref 4a.
(5) Cooper, D. L.; Gerratt, J.; Raimondi, M. In *Advances in the Theory of Benzenoid Hydrocarbons*. Gutman, I., Cyvin, S. J., Eds. *Top. Current Chem.* **1990**, *153*, 41.
(6) Cooper, D. L.; Gerratt, J.; Raimondi, M. *Molecular Simulation* **1990**, *4*, 293.

$$\Psi_{SM} = \sum_{k=1}^{f_S^N} c_{Sk}\mathcal{A}(\Phi\Theta_{SM;k}^N) \quad (3)$$

in which Φ is an N-electron spatial function that does not possess any particular permutational symmetry, $\mathcal{A}$ is the antisymmetrizing operator, and the c_{Sk} may be termed spin-coupling coefficients.

In spin-coupled theory, we approximate the N-electron spatial function with a product of N distinct non-orthogonal orbitals $\phi_\mu(r_\mu)$:

$$\Phi(r_1,r_2,...,r_N) = \phi_1(r_1)\phi_2(r_2)...\phi_N(r_N) \quad (4)$$

The orbitals are expanded in a set of basis functions χ_p

$$\phi_\mu = \sum_p c_{\mu p}\chi_p \quad (5)$$

with no orthogonality constraints whatsoever. All the variational parameters, namely the orbital coefficients $c_{\mu p}$ and the spin-coupling coefficients c_{Sk}, are optimized simultaneously by using an efficient procedure that uses the second derivatives of the total energy. As mentioned earlier, the form of the orbitals is a unique outcome of the energy minimization.

At convergence, it can be shown[10] that each occupied orbital ϕ_μ satisfies an orbital equation of the type

$$\hat{F}_\mu^{(\mathrm{eff})}\phi_\mu = \epsilon_\mu\phi_\mu \quad (6)$$

These effective operators are all distinct, and each gives rise to a set of functions $\phi_\mu^{(i)}$ with orbital energies $\epsilon_\mu^{(i)}$. One of these functions corresponds to the occupied orbital already found, while the others are excited or "virtual" solutions.

The $\hat{F}_\mu^{(\mathrm{eff})}$ operators are constructed from quantities that depend only on $N-1$ electrons, and so the virtual orbitals correspond to the motion of one electron in the field of the other $N-1$ electrons. Consequently, they provide very good descriptions of the behavior of electrons in excited states. These virtual orbitals may be used to form excited spin-coupled structures for use in a subsequent non-orthogonal CI calculation. The final "spin-coupled valence bond" wave function consists of a linear combination of the spin-coupled configuration and a modest list of excited structures. As stressed earlier, the final wave function for the ground state is dominated by the spin-coupled configuration for all nuclear geometries—a similar situation holds for excited states.

Although it is based on just one spatial configuration, the spin-coupled wave function is very flexible. The response of the system to the interactions arising during a chemical reaction is manifested as a modification of the orbitals and as a recoupling of the electron spins. The spin-coupling coefficients are particularly sensitive indicators of changes in the wave function. The spin-coupled VB potential energy surfaces consistently turn out to be parallel to those from very extensive CI calculations. An example that is particularly relevant to the current work is CH_2, where we were able to compare our spin-coupled VB calculations[11] with the full CI calculations of Bauschlicher and Taylor[12] for the $^3B_1$–$^1A_1$ splitting.

IV. Calculations

The methane molecule has ten electrons with a net spin of zero, and this poses no problems for our methods. Calculations have now been completed for a number of singlet systems with ten "active" electrons, such as naphthalene,[13] acetylene, and HCN,[14] using the full spin space of $f_0^{10} = 42$ functions. However, it makes more sense in the present case to include electron correlation effects for the valence electrons but not for the $1s^2$ core electrons on carbon.

In some of our studies of organic π-electron systems[15-17], we have allowed the doubly occupied "core" orbitals to relax, in a self-consistent manner, in the field of the improved description of the active electrons. In each case we found negligible changes in the physical picture, and so we have chosen to "freeze" the $C(1s^2)$ core in the present calculations. Thus, in the present work we have applied spin-coupled theory explicitly only for the eight valence electrons, which we describe by eight distinct non-orthogonal orbitals. The full spin space of $f_0^8 = 14$ functions has been employed.

Starting from tetrahedral methane with a C–H bond length of 2.065 bohr, we first performed a closed-shell Hartree–Fock SCF calculation for each nuclear geometry. The double-ζ plus polarization (DZP) basis set consisted of (9s5p/4s) primitive Gaussian functions contracted[18] to [4s2p/2s], and this was augmented with a d polarization function on carbon with an exponent of 0.78 and a p polarization function on each of the hydrogens with an exponent of 1.0. Spherical Gaussian functions with five d components were used, and so there were 35 basis functions in all. The spin-coupled calculations for the ground state were then carried out with the two core electrons accommodated in the doubly occupied $1a_1$ SCF molecular orbital. The eight singly occupied non-orthogonal spin-coupled orbitals were optimized in the form of completely general linear combinations of the remaining 34 SCF orbitals. The wave function may thus be written

$$\Psi_{SM} = \sum_{k=1}^{14} c_{Sk}\mathcal{A}(1a_1^2\Theta_{00}^2\phi_1\phi_2\phi_3\phi_4\phi_5\phi_6\phi_7\phi_8\Theta_{SM;k}^8) \quad (7)$$

where Θ_{00}^2 is the spin function for two electrons with a net spin of zero.

All the calculations in the present work were carried out in the Rumer basis of spin functions.[19,20] For a system with a net spin of zero, this corresponds to pairing off the individual spins to form singlets in all possible ways, while making use of simple criteria to select a complete linearly independent set.[21] These spin functions, which are used extensively in classical VB theory, are non-orthogonal; this requires a slight modification of the expressions used to compute the weights of the various spin couplings.[22]

Orbital Picture of the Molecular Fragments. We now describe very briefly the spin-coupled wave functions for $CH_2(^1A_1)$, H_2, CH_4, and CH_3, some of which have been discussed in recent publications. The six spin-coupled valence orbitals for $CH_2(^1A_1)$ may be characterized as follows.[11,23] Orbital ϕ_1 is in essence a lobe of an approximately sp^3-like hybrid pointing toward orbital ϕ_2, which is a slightly deformed H(1s) orbital. Orbitals ϕ_3 and ϕ_4 are the counterparts that describe the second C–H bond. Orbitals ϕ_5 and ϕ_6 are the two remaining lobes of the sp^3-like hybrids and describe the nonbonding electrons, with spins coupled to a singlet. The spin-coupled description of the ground state of H_2 is very simple and takes the form of two slightly distorted H(1s) orbitals that overlap strongly with one another.[3]

The eight spin-coupled orbitals for the valence electrons of methane[24] fall into the two groups of four. Four of the orbitals

(7) Wigner, E. P. *Group Theory*; Academic Press: New York, 1959.
(8) Kotani, M.; Amemiya, A.; Ishiguro, E.; Kimura, T. *Tables of Molecular Integrals*, 2nd ed.; Maruzen: Tokyo, 1963.
(9) Gerratt, J. *Adv. At. Mol. Phys.* **1971**, *7*, 141.
(10) Gerratt, J.; Raimondi, M. *Proc. R. Soc. London A* **1980**, *371*, 525.
(11) Sironi, M.; Cooper, D. L.; Gerratt, J.; Raimondi, M. *J. Chem. Soc., Faraday Trans. 2* **1987**, *83*, 1651.
(12) Bauschlicher, C. W.; Taylor, P. R. *J. Chem. Phys.* **1986**, *85*, 6510.
(13) Sironi, M.; Cooper, D. L.; Gerratt, J.; Raimondi, M. *J. Chem. Soc., Chem. Commun.* **1989**, 675.
(14) Sironi, M.; Cooper, D. L.; Gerratt, J.; Raimondi, M. To be submitted for publication.
(15) Cooper, D. L.; Gerratt, J.; Raimondi, M.; Wright, S. C. *Chem. Phys. Lett.* **1987**, *138*, 296.
(16) Cooper, D. L.; Wright, S. C.; Gerratt, J.; Hyams, P. A.; Raimondi, M. *J. Chem. Soc., Perkin Trans. 2* **1989**, 719.
(17) Cooper, D. L.; Gerratt, J.; Raimondi, M. *J. Chem. Soc., Perkin Trans. 2* **1989**, 1187.
(18) Dunning, T. H., Jr. *J. Chem. Phys.* **1970**, *53*, 2823.
(19) Rumer, G. *Göttingen Nachr.* **1932**, 377.
(20) Pauncz, R. *Spin Eigenfunctions*; Plenum: New York, 1979.
(21) Raimondi, M.; Simonetta, M.; Tantardini, G. F. *Comput. Phys. Rep.* **1985**, *2*, 173.
(22) Chirgwin, B. H.; Coulson, C. A. *Proc. R. Soc. London A* **1950**, *201*, 196.
(23) Wright, S. C.; Cooper, D. L.; Sironi, M.; Raimondi, M.; Gerratt, J. *J. Chem. Soc., Perkin Trans. 2* **1990**, 369.

are localized on hydrogen. They all have the same orbital energy, as defined by eq 6, and they can be transformed into one another by symmetry operations of the T_d point group. Another set of four degenerate orbitals is localized on carbon. Each of them resembles an approximately sp^3-like hybrid pointing toward one of the H atoms. The other orbitals are identical in shape and are related to this one by molecular symmetry operations. The perfect-pairing function is the dominant mode of spin coupling, but there are also small contributions from all of the others. Contrary to the *assumptions* in classical VB theory, these four hybrids are not orthogonal to one another. However, each of them overlaps most strongly only with the hydrogen orbital to which it points, and the dominant mode of spin coupling corresponds to four equivalent C–H bonds. Both sets of orbitals carry *reducible* representations of the molecular point group, but the total wave function transforms as the A_1 irreducible representation of the T_d point group, as it should. We have shown how the photoelectron spectrum of methane can be interpreted in terms of spin-coupled theory.[24]

The picture of the $^1A_1$ state of CH_2 differs markedly from that afforded by molecular orbital theory, according to which the two nonbonding electrons occupy a single lobe of what is essentially a $C(sp^2)$ hybrid. It is worth pointing out that a GVB calculation by Goddard and co-workers[25] gives rise to a view of $CH_2(^1A_1)$ that is fairly similar to that offered by the spin-coupled wave function. However, the orbitals in the GVB method are subject to the "strong orthogonality" constraint, and only one mode of spin coupling is included, corresponding to singlet coupling of the electrons in each pair. As a result of these constraints, it is not possible within the perfect-pairing GVB model to contemplate the study of the singlet methylene insertion reaction $CH_2(^1A_1) + H_2 \rightarrow CH_4$.

Finally, we describe the seven valence orbitals of the CH_3 fragment. Three of them are found to be essentially distorted 1s functions localized on the hydrogen atoms; they are degenerate and are transformed into one another by symmetry operations of the D_{3h} point group. Each of these orbitals overlaps strongly with one member of another set of three degenerate orbitals. Not surprisingly, the orbitals in the second set are perfectly recognizable as essentially sp^2 hybrids on carbon, and they are transformed into one another by successive $\hat{C}_3$ rotations. The seventh orbital is invariant under all of the C_{3v} symmetry operations and is not related to any of the others—it possesses $C(p_\pi)$ character.

The three sp^2-like orbitals on the carbon atom in CH_3 are not orthogonal to one another, and all of the orbitals show some distortion toward neighboring atoms.

Description of the Cuts of the Potential Surfaces. For the hydrogen atom abstraction reaction $CH_4 \rightarrow CH_3(^2A_1') + H$, we have concentrated on a least-motion path, starting from the equilibrium geometry of methane. One C–H bond was stretched, keeping all the other separations in the CH_3 pyramidal fragment fixed at their values in CH_4.

This portion of the surface has been investigated by many authors. In particular, Hirst[26] has determined a minimum energy path by optimizing, at the MRDCI level of theory, the umbrella angle of CH_3 as a function of the distance from the hydrogen atom. This portion of the surface has also been studied more recently with coupled cluster methods.[27] We did not perform additional calculations along the C_{3v} minimum energy path, which exhibits no activation barrier, as there are no particular effects to be expected beyond correcting for the wrong asymptotic behavior of the restricted Hartree–Fock solution. The description of this process is essentially trivial for spin-coupled theory.

At the molecular level the process is characterized by the conversion of an sp^3-like hybrid into an sp^2-like hybrid localized on carbon. This process occurs simultaneously with the weakening of the C–H bond involving the departing hydrogen atom. This is illustrated in Figure 1 by the variation of the overlap between the two relevant spin-coupled orbitals as a function of the bond distance. The spin-coupling coefficients do not manifest any physically significant change: the perfect-pairing spin function remains the most important (>90%) over the entire range of bond distances, although there are also contributions from all of the others.

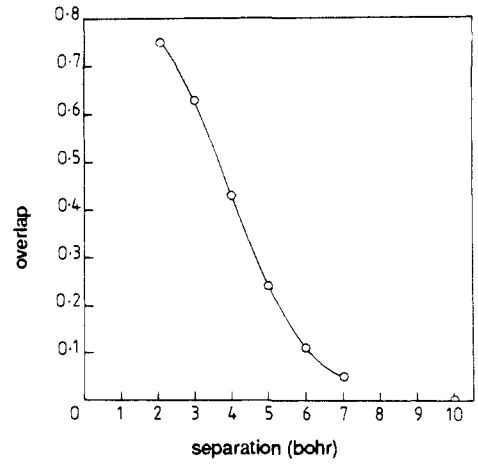

Figure 1. Overlap between the spin-coupled orbitals involved in the bond-breaking process $CH_4 \rightarrow CH_3(^2A_1') + H$.

One spin-coupled orbital is perfectly localized on the departing hydrogen atom and has H(1s) character. The orbitals localized on the CH_3 fragment evolve into those of the $CH_3(^2A_1')$ radical described above.

For the reaction $CH_2(^1A_1) + H_2 \rightarrow CH_4$, we have considered a number of cuts through the potential surface. First of all, we concentrated on least-motion paths within C_{2v} symmetry as suggested by the orbital pictures of CH_2, H_2, and CH_4. We then extended our investigation to a non-least-motion path, inspired by the principle of maximum overlap between the relevant spin-coupled orbitals and by the experience gained during the spin-coupled study of the cycloaddition reaction of $CH_2(^1A_1)$ with ethene.[11]

In this new pathway, the initial approach of H_2 to CH_2 is with the H–H bond pointing along the direction of one of the nonbonding sp^3-like spin-coupled orbitals of methylene. At the same time, the hydrogen atom furthest from the CH_2 fragment is free to swing round toward the second nonbonding spin-coupled orbital. In this way, the formation of the first new C–H bond occurs directly, while the second bond develops more gradually and simultaneously with the weakening of the H–H bond. It is evident that this path differs conceptually from the non-least-motion path determined by Bauschlicher et al.[28] in which the H–H axis is parallel to the plane of the CH_2 fragment—this trajectory was suggested by the MO picture of $CH_2(^1A_1)$, in which the HOMO is a nonbonding sp^2-like hybrid and the LUMO is essentially a $C(2p_\pi)$ orbital that can interact favorably with the HOMO of H_2.

It is important to note that we include all 14 allowed spin functions. At the equilibrium nuclear geometry of methane, the wave function is dominated by just one of these modes of spin coupling, namely the one corresponding to four C–H electron-pair bonds. However, as soon as we move away from equilibrium geometry, as considered below, other spin functions start to play a more significant role. Indeed, they are *essential* in allowing the electrons to decouple from one another as one bond breaks and to recouple as new bonds form.

V. Results

We are now in a position to examine the overall orbital picture for the chemical reaction $CH_2(^1A_1) + H_2 \rightarrow CH_4$ as revealed by

(24) Penotti, F.; Cooper, D. L.; Gerratt, J.; Raimondi, M. *J. Mol. Struct. (THEOCHEM)* **1988**, *169*, 421.
(25) Hunt, W. J.; Hay, P. J.; Goddard, W. A., III *Chem. Phys.* **1972**, *57*, 738.
(26) Hirst, D. M. *Chem. Phys. Lett.* **1985**, *122*, 225.
(27) Sosa, C.; Noga, J.; Purvis, G. D.; Bartlett, R. J. *Chem. Phys. Lett.* **1988**, *153*, 139.
(28) Bauschlicher, C. W.; Haber, K.; Schaefer, H. F., III; Bender, C. F. *J. Am. Chem. Soc.* **1977**, *99*, 3610.

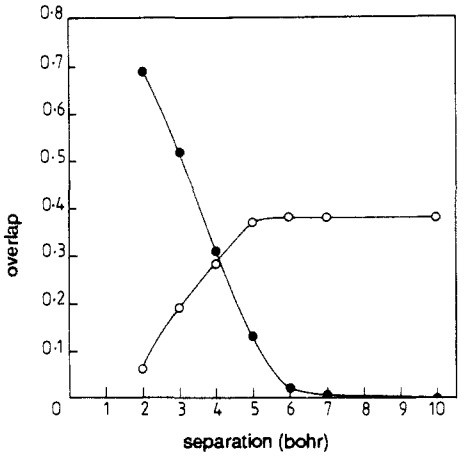

Figure 2. C–H (●) and H–H (○) overlaps for the process $CH_2(^1A_1) + H_2 \rightarrow CH_4$ (C_{2v} least-motion path).

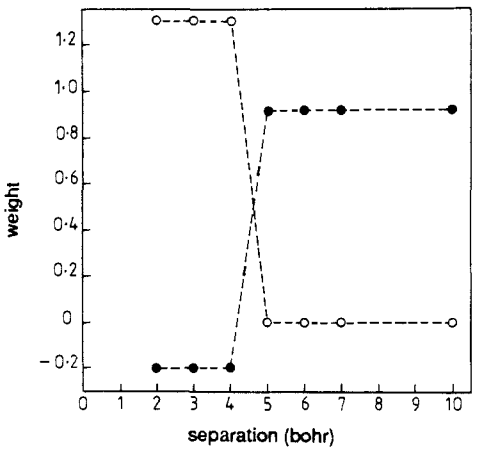

Figure 3. Weights of the two most important spin couplings as a function of the distance between CH_2 and H_2 (C_{2v} least-motion path). The two spin functions are (○) four C–H bonds and (●) two C–H bonds (on CH_2), with singlet coupling of the nonbonding electrons on CH_2 and one H–H bond.

spin-coupled theory. After optimizing the geometries of the reactants, we compute an exothermicity for this process of 113.4 kcal mol^{-1}. This may be compared with the value of 117 kcal mol^{-1} obtained by adding the best current estimate for the $^3B_1$–$^1A_1$ separation of 9 kcal mol^{-1} to the known value[29] of 108 ± 1 kcal mol^{-1} for the ground-state process $CH_2(^3B_1) + H_2 \rightarrow CH_4$.

Bauschlicher et al.[30] computed a barrier height of 26.75 kcal mol^{-1} for the direct C_{2v} approach. This is in qualitative agreement with orbital symmetry arguments, according to which the process is forbidden. However, as pointed out by Silver and Karplus,[31] the application of the rules of Woodward and Hoffmann[32] to predict the stereospecific course of reactions is based on the assumption that a single configuration is dominant in the MO theory wave function. This is not the case for singlet methylene, where at least two configurations are required in MO theory. Experiments have established that singlet methylene reacts with molecular hydrogen with little or no activation energy.[29a]

We now describe our results for the C_{2v} cut through the surface $CH_4 \rightarrow CH_2(^1A_1) + H_2$ in which the H–H fragment is removed with the interatomic distance fixed at its value in CH_4. This illustrates the insight that is provided by the spin-coupled wave function, even though the path is not particularly favorable from an energetic point of view.

Inspection of the spin-coupled orbitals shows that the four valence orbitals of carbon conserve their essential character of sp^3-like hybrids along the whole path, and similarly the other orbitals remain localized on the hydrogen atoms. The distortions developing during the course of the reaction are such that the overlaps of the orbitals involved in the bond-breaking and bond-forming process change smoothly, though constantly, from the regime of the reactants to that of the products. This is illustrated in Figure 2 where we show the C–H and H–H overlaps. The changes in the spin-coupling coefficients go together with those of the overlaps between the different orbital pairs and reveal much about the nature of the process leading to the formation of the new chemical bonds.

In the regions of the reactants, the spin couplings correspond to bonds localized on the molecular fragments. Once past the barrier, the mode of spin coupling changes dramatically and the new C–H bonds characteristic of methane appear to be formed in a single step. In Figure 3 we show the weights of the two most important spin couplings as a function of the distance between CH_2 and H_2; the recoupling occurs in a narrow range of interfragment distances, corresponding to the region of the barrier.

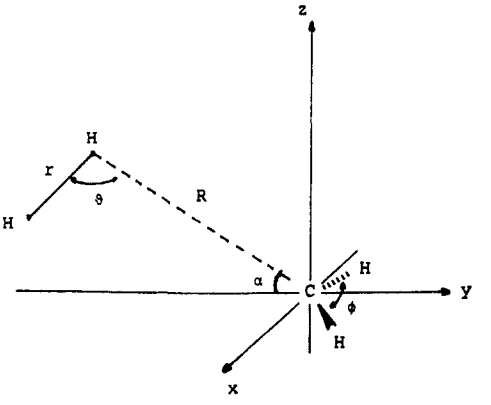

Figure 4. Geometrical parameters optimized in the new minimum energy path. The H–H molecule is in the *yz* plane.

Table I. Minimum Energy Path for the Reaction $CH_2(^1A_1) + H_2 \rightarrow CH_4$[a]

R/bohr	r/bohr	ϑ, deg	ϕ, deg	α, deg	energy/hartree
3.0	2.92	46.0	146.9	30.0	−40.1870
3.6	1.46	223.1	107.1	81.9	−40.1864
4.5	1.47	207.5	105.9	86.0	−40.1850
15.0	1.45	205.9	105.9	47.2	−40.1845

[a] The various parameters are defined in Figure 4.

In the transition region, where both of these modes of spin coupling contribute, we notice a tendency for the orbitals of H_2 to delocalize toward the CH_2 fragment, while those of CH_2 overlap significantly with two partners, a hydrogen orbital and a methylene orbital.

Finally, we consider the new minimum energy pathway for the singlet methylene insertion reaction suggested by the spin-coupled orbital description of $CH_2(^1A_1)$. As described above, the initial approach of H_2 is with its bond axis pointing along the direction of one of the nonbonding spin-coupled orbitals—the H atom furthest from the CH_2 fragment is free to locate itself in the most favorable position, in a plane perpendicular to the CH_2 molecule and bisecting the HCH angle. In order to take advantage of all the results obtained in the detailed studies of Bauschlicher et al.,[28,30] we first carried out MO–CI calculations with the same [4s2p/2s] DZ basis set and the same list of configurations as used by those authors. The CI wave function involved all single and double excitations out of a two-configuration SCF wave function.

Figure 4 identifies the geometrical parameters α, ϑ, r, and R used to define a particular trajectory—the minimum energy path found by Bauschlicher et al.[28] corresponds to fixing the values of α and ϑ at 90°. We optimized α, ϑ, ϕ, and r for each different

(29) (a) Kirmse, W. *Carbene Chemistry*, 2nd ed.; Academic Press: New York, 1971. (b) Stull, D. R.; Prophet, H. In *JANAF Thermochemical Tables*, 2nd ed.; National Bureau of Standards: Washington, DC., 1971.
(30) Bauschlicher, C. W.; Schaefer, H. F., III; Bender, C. F. *J. Am. Chem. Soc.* **1976**, *98*, 1653.
(31) Silver, D. M.; Karplus, M. *J. Am. Chem. Soc.* **1975**, *97*, 2645.
(32) Woodward, R. B.; Hoffmann, R. *J. Am. Chem. Soc.* **1965**, *87*, 395, 2046, 2511.

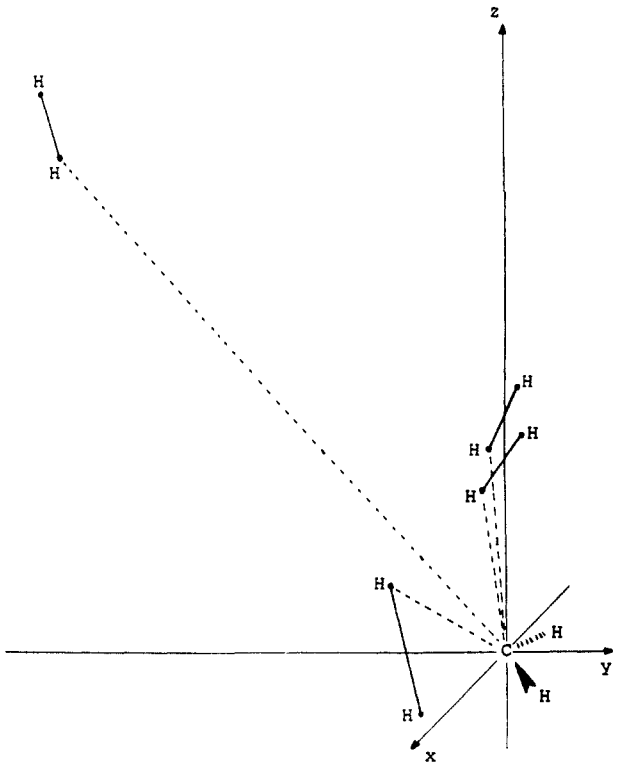

Figure 5. Arrangements of the CH_2 and H_2 fragments at the optimal geometries reported in Table I.

value of R and were able to find a new path with no barrier. An analogous calculation based on our DZP basis set confirmed that this path has no barrier. We report in Table I the values of the geometrical parameters corresponding to the lowest energy at a given value of R (see also Figure 5). It is apparent that this new minimum energy path differs markedly from that found by Bauschlicher et al.[28]

At R = 15 bohr, the H_2 molecule approaches methylene with one H atom moving along a direction close to that defined by the classical sp^3 hybrid of CH_4. The other H atom is not significantly attracted by the other sp^x-like hybrid of CH_2, and its location is determined by minimizing the repulsions.

At R = 4.5 bohr, the angle α increases to $\approx 86°$, but the H_2 molecule is not parallel to the plane of CH_2. At R = 3.6 bohr, α decreases to $\approx 82°$ but r is still close to the bond length in the H_2 molecule.

At R = 3.0 bohr, all the major changes have occurred: α is 30°, r is 2.92 bohr (and approaches the value of the H–H distance in CH_4), and ϑ is $\approx 46°$, so that the second H atom now points toward the other sp^3-like hybrid of CH_2.

In spite of the large changes in the conformation of the molecule along this trajectory, the changes in the spin-coupled orbitals are fairly modest, although very interesting.

As the two fragments come together, the slightly distorted H(1s) orbitals overlap less strongly with one another (see Figure 6a), and distort instead toward the carbon atom, as shown in Figure 6b. The nonbonding hybrids on CH_2 are already of essentially the correct form for making two new C–H bonds in methane. However, as illustrated by Figure 6c, they are polarized and distorted toward the more distant hydrogen atom, sometimes assuming very peculiar shapes.

As was the case for the energetically unfavorable C_{2v} least-motion path, we can conclude that the changes in the spin-coupling coefficients are much more fundamental to the reaction than are any modifications of the orbitals.

VI. Discussion and Comparison with Classical VB Theory

The spin-coupled description of the valence electrons in methane, singlet methylene, and the methyl radical coincides fairly closely with the conventional intuitive chemical view of localized C–H bonds. Everywhere on the surfaces, four of the orbitals are localized on hydrogen and resemble atomic 1s functions. The other four orbitals are localized on carbon, and each points toward a hydrogen atom or accommodates a nonbonding electron: they are very similar to Pauling's picture[33] of either sp^3 or sp^2 hybrids. However, none of the orbitals is orthogonal to any of the others. Furthermore, all of the orbitals show some distortion toward neighboring atoms, and this has the important consequence that structures involving charge separation (i.e. "ionic" structures) are unimportant.

In the asymptotic region of the reactants, the spin pairing and the overlaps show bonds localized on the molecular fragments. As the fragments approach one another, the spin pairing and the overlaps change, and the new C–H bonds are formed. The orbitals localized on the fragments are distorted when the fragments come together, the distortion being greatest in the regions where new bonds are formed, and there are points on the surface where there is some delocalization of the orbitals.

According to the Weyl formula, there are 485 649 472 classical VB structures for a system of 8 electrons and 34 orbitals (DZP basis with a frozen core), and this gives some idea of the computational complexity that has to be overcome. In spite of the availability of highly efficient modern algorithms,[2,34] a classical VB calculation using all of these structures is currently out of the question.

Only the introduction of hybrids allows us to consider classical VB wave functions that are compact enough to make the calculations feasible with an extended basis set. However, when studying a chemical reaction, there is the additional puzzle of choosing a single set of hybrids that is appropriate everywhere on the surface. In a detailed study of the $CH_2(^1A_1) + H_2 \rightarrow CH_4$ and $CH_4 \rightarrow CH_3(^2A_1') + H$ surfaces with classical VB theory,[35] sp^3 hybrids were constructed by combining SCF orbitals calculated with a basis set of DZ quality. In spite of the evidently inappropriate choice of sp^3 hybrids to describe planar $CH_3(^2A_1')$, it proved possible to select a rather compact set of structures but it was not possible to attain sufficient quantitative accuracy.

VII. Summary and Conclusions

Spin-coupled theory is based on an orbital picture with one orbital for each electron, and with all possible modes of coupling together the spins of the electrons. The orbitals are expanded in a basis set and are fully optimized, together with the weights of the different spin couplings. No preconceptions or orthogonality constraints whatsoever are imposed, and the form of the orbitals is a *unique* outcome of the energy minimization. The spin-coupled wave function provides a highly visual model of the behavior of *correlated* electrons. Subsequent non-orthogonal CI calculations, which transcend the orbital approximation and which include further electron correlation effects, have not been performed here, as all our experience to date shows that they would not change the essential physical picture. This study has shown how the electronic structure of the processes $CH_2(^1A_1) + H_2 \rightarrow CH_4$ and $CH_4 \rightarrow CH_3(^2A_1') + H$ can be interpreted in terms of simple and consistent orbital pictures that include electron correlation effects from the outset.

The overall descriptions of these reactions are quite different from the usual ones based on MO theory. In particular, our results indicate that the change of spin coupling is fundamental in characterizing what might be termed the "act of reaction".

Concepts such as localized bonds, hybridization, and nonbonding orbitals, which are invaluable for organizing our knowledge of electronic structure and chemical reactivity and for allowing us to make reliable predictions, have been proved to be the direct outcome of purely ab initio calculations without preconceptions.

The determination of minimum energy paths, and the location of barriers along them (if any), usually calls for extensive search procedures. A key feature of the current work is the *guidance*

(33) Pauling, L. *Proc. Natl. Acad. Sci. U.S.A.* **1928**, *14*, 359; Pauling, L. *J. Am. Chem. Soc.* **1931**, *53*, 1367.
(34) Raimondi, M.; Gianinetti, E. *J. Phys. Chem.* **1988**, *92*, 898.
(35) Raimondi, M. *Report of Workshop on Collisions, Centre European de Calcul Atomique et Moleculaire*); CECAM: Orsay-Paris, 1975.

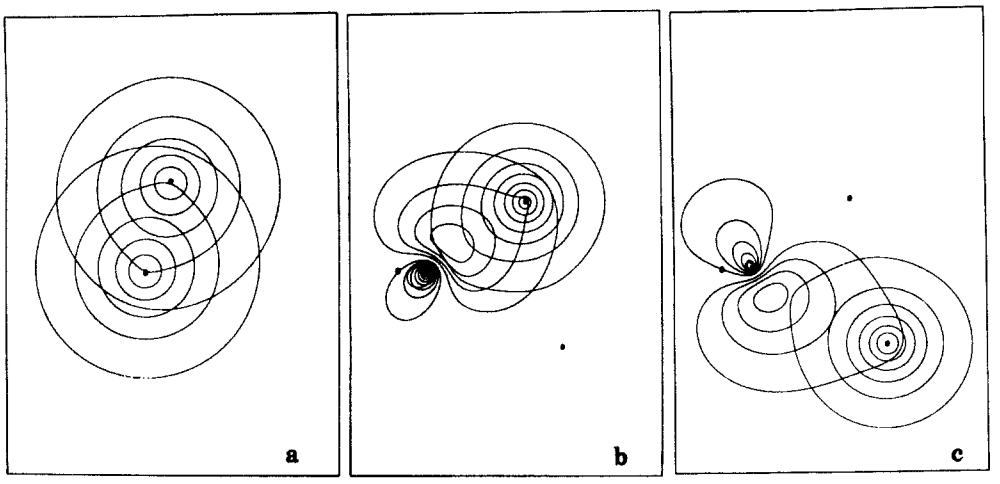

Figure 6. Superimposed contour plots of spin-coupled orbitals: (a) the H-H bond at R = 15 bohr; (b) the first C-H bond at R = 3.0 bohr; (c) the second C-H bond at R = 3.0 bohr.

provided by valence theory, in its proper form, as to which portions of the potential surface should be searched.

Further calculations require larger basis sets and wave functions that take better account of correlation effects over the entire surface. The use of the virtual orbitals generated by spin-coupled theory will allow us to generate a compact set of valence bond structures and, at the same time, to obtain results accurate enough to justify a subsequent dynamical study of the reaction. In particular, we intend to pursue further the approach of H_2 to CH_2 along the direction of one of the nonbonding sp^3-like orbitals.

An MP2 and MCSCF/CI Study of the Aluminum–Acetylene Adducts†

John S. Tse

Contribution from the Division of Chemistry, National Research Council of Canada, Ottawa, Ontario, Canada K1A 0R9. *Received August 11, 1989*

Abstract: The $\sigma \rightarrow \pi$ conversion of aluminum–acetylene adducts have been examined with ab initio calculations. Contrary to previous studies, the σ-bonded cis adduct was found to be unstable when electron correlations in the valence space were taken into account. Geometry optimization with the MP2 and (CAS)MCSCF methods starting at the cis conformation always converged to a symmetric (π) complex with a $^2B_2$ ground state. A second shallow minimum, separated from the first one by a small potential barrier, was located along the symmetric direction at large Al–C_2H_2 distances by the CASSCF calculations. However, both the barrier and the minimum disappeared when the dynamical correlation effect was included. The $^2A'$ σ-bonded *trans*-aluminoacetylene remained a stable adduct.

1. Introduction

Reactions of unsaturated hydrocarbons with aluminum have a very rich and interesting chemistry. Many organoaluminum complexes can be isolated at low temperature in inert matrices by cocondensation of the metal with excess unsaturated hydrocarbon.[1-6] These adducts are very reactive and useful as catalysts for polymerization reactions.[3-5] Recently, the heat of association of the aluminum atom with simple alkynes and arenes in the gas phase at room temperature has been obtained directly from time-resolved resonance fluorescence experiments.[7] So far, the aluminum adducts of acetylene and ethylene have received the most attention.

There are two possible isomers for the acetylene adduct. The aluminum atom can bond to a single carbon, forming the σ complex, or it can bond to two carbon atoms in the symmetric C_{2v} position. In Al–ethylene, in addition to the symmetric or π conformation, the Al–C bond can either be trans or cis to the unpaired electron on the neighboring carbon atom. Experimental ESR studies suggested that Al–C_2H_2 is a σ adduct whereas Al–C_2H_4 is a symmetric π complex.[1,2,5] The unexpected difference in the mode of chemical bonding between the acetylene and ethylene complexes has generated a great deal of theoretical interest in these systems. Geometry optimizations at the Hartree–Fock level employing double-ζ basis sets show that the σ adducts are the most stable structures for both the acetylene[8,9] and ethylene adducts[10] and the π conformers are the transition

† Published as NRCC 31465.

(1) Kasai, P. H.; McLeod, D., Jr.; Watanabe, T. *J. Am. Chem. Soc.* **1977**, *99*, 3521.
(2) Kasai, P. H. *J. Am. Chem. Soc.* **1982**, *104*, 1164.
(3) Chenier, J. H. B.; Howard, J. A.; Tse, J. S.; Mile, B. *J. Am. Chem. Soc.* **1985**, *107*, 7290.
(4) Chenier, J. H. B.; Howard, J. A.; Mile, B. *J. Am. Chem. Soc.* **1987**, *109*, 4109.
(5) Howard, J. A.; Mile, B.; Tse, J. S.; Morris, H. *J. Chem. Soc., Faraday Trans. 1* **1987**, *83*, 3701.
(6) Howard, J. A.; Mile, B.; Tse, J. S. *Organometallics* **1988**, *7*, 128.
(7) Mitchell, S. A.; Simard, B.; Rayner, D. M.; Hackett, P. A. *J. Phys. Chem.* **1988**, *92*, 1655.
(8) Trenary, M.; Casida, M. E.; Brooks, B. P.; Schaefer, H. F. *J. Am. Chem. Soc.* **1979**, *101*, 1638.
(9) Scheiner, A. C.; Schaefer, H. F. *J. Am. Chem. Soc.* **1985**, *107*, 4451.

0002-7863/90/1512-5060$02.50/0 Published 1990 by the American Chemical Society